Numerical studies of the effects of design parameters on flow fields in spiral concentrators

Numerical studies of the effects of design parameters on flow fields in spiral concentrators

Guichuan Ye[a,b], Liqiang Ma[a], Federico Alberini[b], Qian Xu[c], Gen Huang[a], and Yuexian Yu[a]

[a]School of Chemical & Environmental Engineering, China University of Mining & Technology (Beijing), Beijing, China; [b]School of Chemical Engineering, University of Birmingham, Birmingham, UK; [c]School of energy and environmental engineering, University of Science & Technology Beijing, Beijing, China

ABSTRACT

Spiral concentrators are widely used for the concentration of coal and heavy minerals. The design for the spiral concentrator is full of challenge because of the sensitivity of design parameters to water flow field. The study aims to reveal the rule of the design parameters on water flow field in spiral concentrators. The pitch, the transverse angle, and the flow rate were taken as the variables. A suggested simulation method based on grid independence investigation, four types of turbulence models, and Volume of Fluid (VOF) approach was proposed. The water flow field on spirals with different design parameters was determined by the validated model. The predicted water flow depth show agreement with the measured results. The Reynolds-Stress Model (RSM) turbulence model is superior to other turbulence models. The water depth and the primary velocity in spiral concentrators increase smoothly outward. The secondary velocity is relatively small compared with the primary velocity. No obvious secondary flow exists in the inner trough. The reversal position of the secondary flow is approximate at the fractional depth of 0.2 ~ 0.5. The reduction of the pitch and the flow rate, together with the increase of the transverse angle, can strengthen the secondary flow in spiral concentrators.

Introduction

The spiral concentrator has been widely used to separate the valuable minerals from the gangue particles based on the differences in particle density (Holland-Batt 1995; Kwon et al. 2017). During the last decades, applications and optimizations of spiral concentrators have been developed, bringing with the advantages of simplicity of operation, low energy consumption, and high efficiency. The spiral concentrator consists of an open trough, which spirals vertically downwards in a helix configuration around a central axis (Matthews, Fletcher, and Partridge 1998). Despite its apparent simplicity, the separation mechanism is complex. Mishra developed a simulation tool based on the discrete element method (DEM) to understand the separation process in spiral concentrators (Mishra and Tripathy 2010). Jihoe simulated the particle flow in a Humphrey spiral concentrator using the extended smoothed particle hydrodynamics (SPH) model (Kwon et al. 2017). Boucher studied the particle motion ina spiral concentrator using the Positron Emission Particle Tracking (PEPT) technique.

2016b, 2016a). Kapur and Das proposed the mathematic models for the particle radial location on the trough according to their size and density, assuming that the particles eventually reached a dynamic equilibrium both in the forward longitudinal direction and static in the transverse direction (Das et al. 2007; Kapur and Meloy 1998). Besides, numbers of traditional separation experiments were also conducted to explore the particle distribution in spiral concentrators (Bazin et al. 2014; Dehaine and Filippov 2016; Dixit et al. 2015; Grobler 2017; Li, Wood, and Davis 1993; Palmer 2016; Tripathy and Rama Murthy 2012). The previous studies above have revealed that the heavy particles prefer to move inward, while the light particles tend to be placed in the outer trough. The water flow field, as the basis of the particle separation in spiral concentrators, has been reported extensively.

As reported, the flow pattern in a spiral concentrator consisted of a primary (down trough) flow component with a secondary (transverse) circulation superimposed (Holland-Batt 1989). Holland-Batt and Loveday presented that the water depth in spiral concentrators increased radially (Holland-Batt 1989; Loveday and Cilliers 1994). Holtham showed evidence of the secondary flow in spiral concentrators by capturing the image of the streamline of the dye on the trough bottom (Holtham 1990a). It was accepted that the secondary flow patterns played a key role in the particle distribution cross the trough (Holtham 1992; Jain and Rayasam 2017). The previous studies have shown the general flow patterns in spiral concentrators. However, limited details of water flow field in spiral concentrators were exhibited on the basis of the traditional experiments.

The mathematical models were also developed based on fluid mechanics to study the characteristics of water flow filed in spiral concentrators (Holland-Batt 1989, 2009; Loveday and Cilliers 1994). For example, Holland–Batt provided an approximate modelof the fluid dynamics of slurries using the Manning equation for the primary flow in the inner region and the free vortex equation for the flow in the outer region (Holland-Batt 1989). These mathematical models could hardly realize the visualization of the water flow field. Besides, the relevant models were established by some ideal assumptions, which has some limitations to predict the real flow filed of spiral concentrators.

To overcome the drawbacks above, the computational fluid dynamics (CFD) method was used to predict the water flow field in spiral concentrators. The CFD method has shown its superiority in the prediction of flow filed in lots of engineering applications though it was also defective to present the real flow field (Ganegama Bogodage and Leung 2015; Song et al. 2015; Wadnerkar et al. 2016). Wang first drew an outline of the numerical method to find the fully developed laminar flow of a Newtonian liquid on the spiral concentrator (Wang and Andrews 1994). Matthews then simulated the fluid flows on one operational spiral unit, taking the air phase into consideration to trace the air-water surface (Matthews, Fletcher, and Partridge 1998; Matthews et al. 1999). Subsequently, Doheim expended the simulation method based on the volume of Fluid (VOF) approach and periodic boundary conditions (Doheim et al. 2008). In general, the distribution of water depth and the existence of the secondary flow in spiral concentrators have been predicted successfully (Arnold, Stokes, and Green 2014; Doheim et al. 2008; Matthews, Fletcher, and Partridge 1998; Matthews et al. 1999; Wang and Andrews 1994). However, further details of the flow field, especially for the secondary flow characteristics, have not been discussed numerically before. Additionally, the interactions between the design factors and the water flow field were still not revealed.

In this paper, the CFD method was used to understand the complex interactions between the design factors and the fluid flow in spiral concentrators. The mesh

independence study was conducted to determine the optimal grid cells. The water depth of the LD-9 spiral concentrator was regarded as the criterion for the assessment of the simulation results with four turbulence models. The details of the water flow filed were discussed. The validated model was then further extended to simulate the spiral concentrators with different design parameters. The model predictions were analyzed to revealthe influence of the design factors, such as the pitch, flow rate, and transverse angle of the trough, on water flow field in spiral concentrators.

Numerical Simulation

Geometry Models

The geometry models were based on the LD-9 spiral concentrator. The pitch, flow rate, and transverse angle were defined as the variables. The inner and outer radii were fixed at 70 mm, 350 mm, respectively. Nine numerical experiments were conducted. The details of the parameters used in simulations are shown in Table 1.

Computation of the Grid

Geometry models were generated by ANSYS Design Modeler 16.1, and meshing was developed by ANSYS ICEM 16.1. The spiral concentrator was constructed to be the three-dimensional computational domain. Grid independence study was important to gain the reliable results (Xu, Feng, and Zhang 2017a, 2017b). One-fourth turn of the spiral concentrator was considered for the grid independence investigation. The predicted tangential velocities of the water-free surface, using computational grids with 21000,45000, 86000, 126000, 167000, and 207000 cells, respectively, are presented in Fig. 1 (a). As shown in Fig. 1 (a), the grid size has little effect on the simulation results when the grid number was beyond 126000.

The water depth in spiral concentrator was relatively shallow compared with the mainstream length of the spiral concentrator (Doheim et al. 2008; Holland-Batt 1989; Loveday and Cilliers 1994; Matthews, Fletcher, and Partridge 1998). It was inefficient to model the spiral concentrator with 5 or more turns at once. Hence, simulation with one complete turn of the spiral trough was suggested by Doheim (Doheim et al. 2008; Matthews et al. 1999). The periodic boundary condition was used by progressively feedingthe results from the outlet cells back to the inlet until the fully developed conditions

Table 1. Parameters used in simulations.

	Variables		
Conditions	The ratio of the pitch to diameter	Flow rate Q, m^3/h	Transverse Angle β,°
1	0.60	8	26.5
2	0.50	8	26.5
3	0.39	8	26.5
4	0.35	8	26.5
5	0.39	6	26.5
6	0.39	4	26.5
7	0.39	6	21.0
8	0.39	6	16.0
9	0.39	6	11.0

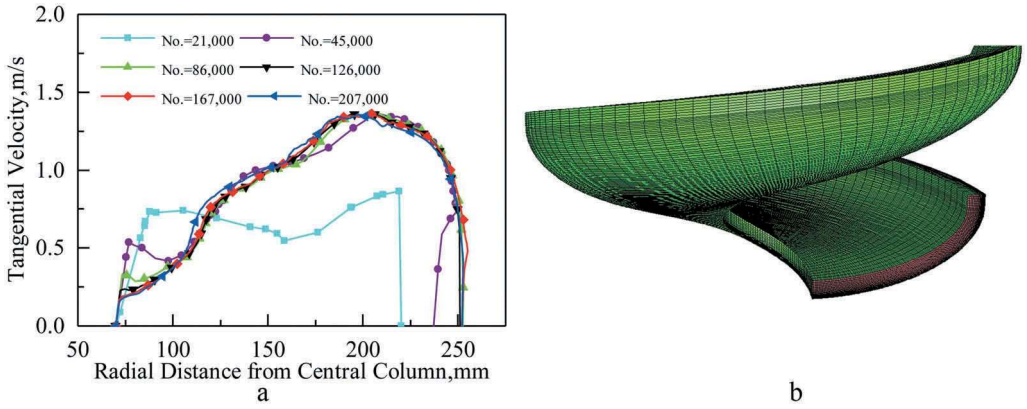

Figure 1. Results of mesh independence (a) and Computational grid (b).

(Doheim et al. 2008). Figure 5(b) shows the suggested computational domain of one complete turn with 105 × 160 × 30 cells in the mainstream, cross-stream, and depth-wise directions, respectively. Since the water flow depth near the trough was even below 1 mm (Holland-Batt 1989), the meshes near the trough bottom were densified to make sure the grids were enough to calculate the flow field even in the shallow position. More specifically, there were 10 layers of grids within 1 mm near the trough.

Free-Surface Treatment and Governing Equations

Free-Surface Treatment

The Volume of Fluid (VOF) approach was used to model the free-surface flow in spiral concentrators. The water free-surface was captured by tracking the interface between the water phase and the air phase. The VOF approach, devised by Hirt and Nichols, can simulate two or more immiscible fluids by solving a single set of momentum equationsand tracking the volume fraction of each fluid in the simulation domain (Hirt and Nichols 1981).

The geometric reconstruction generalized by Youngs (Youngs 1982) was applied in the present study. It assumed that the portion of an interface in a cell was approximated by a straight line, and some satisfactory prediction results had been achieved based on this assumption (Youngs 1982).

Continuity Equation (DOHEIM ET AL. 2008)

The continuity equation for the volume fraction of the phases is given by

$$\frac{@}{@t}\ \alpha_q\rho_q\ \ \text{Þ}\ div\ \ \alpha_q\rho_q\text{ŧ}_q\ \ \text{¼}\ 0 \tag{1}$$

where α is the volume fraction, q is the fluid phase, ρ is the fluid density, u_q is the velocity vector. The volume fractions of all phases can be expressed as follows:

$$\sum_{q=1}^{n} \alpha_q = 1 \tag{2}$$

The volume-fraction-averaged density for an n phase system can be calculated as follows:

$$\sum_{q=1}^{n} \alpha_q \rho_q = \rho \tag{3}$$

Momentum Equation

The momentum equation (4) depends on the volume fractions through the properties ρ and μ (Doheim et al. 2008; Matthews, Fletcher, and Partridge 1998).

$$\frac{\partial}{\partial t}(\rho \vec{v}) + \nabla \cdot (\rho \vec{v}\vec{v}) = -\nabla p + \nabla \cdot [\mu_t (\nabla \vec{v} + \nabla \vec{v}^T)] + \rho \vec{g} + \vec{F} \tag{4}$$

where μ_t is the turbulent viscosity that is given as follows:

$$\mu_t = \rho C_\mu k^2 / \varepsilon \tag{5}$$

$\vec{F}$ is the force vector. It has the following simplified form (Brackbill, Kothe, and Zemach 1992),

$$\vec{F} = 2\sigma_{ij}\rho\psi_i \nabla \alpha_i / (\rho_i + \rho_j) \tag{6}$$

where σ is the surface tension coefficient.

Turbulence Model

The turbulence models, applied in our simulation work, were the standard k-ϵ model, the renormalization group (RNG) k-ϵ model, the shear-stress transport (SST) k-ω model, and the Reynolds-stress model (RSM). Details of these four turbulence models have been described in references (Doheim et al. 2008, 2013; Matthews, Fletcher, and Partridge 1998, 1999).

Boundary Conditions

The computational domain was surrounded by four boundaries, namely: inlet plane, outlet plane, trough wall, and up-wall. At the inlet of the spiral, the velocity componentwas specified by the flow rate. At the outlet plane, the pressure-out conditions were used. At the trough wall, no-slip and no-penetration conditions were considered. Standard wall functions were considered to specify wall boundary conditions. The trough wall-roughness constant was set to 0.5. The up-wall was assumed to be the free-slip conditions.

Initially, the computation domain was patched with air phase only. The water phase flowed into the trough from the inlet plane. After the water has been fully spread out at the outlet, the periodic boundary condition was established to obtain the stable flow field. The results from the outlet cells were progressively feeding back to the inlet cells until fully developed conditions are reached. Phases used in simulation works are assumed to have

the constant physical properties. Thus, the assumed properties are $\rho_{water} = 1 \times 10^3$ kg/m^3, $\mu_{water} = 9 \times 10^{-4}$ kg/ms, $\rho_{air} = 1.225$ kg/m^3, and $\mu_{air} = 1.7894 \times 10^{-5}$ kg/ms.

Numerical Treatment

Simulations were performed by ANSYS FLUENT 16.1. The Pressure-Implicit with Splitting of Operators (PISO) algorithm was used for pressure-velocity coupling. The Pressure Staggering Option (PRESTO) was chosen for pressure interpolation scheme. The Geo-Reconstruct was used for VOF scheme. The Quadratic Upwind Interpolation (QUICK) scheme was applied for the momentum, turbulent kinetic energy equations, and turbulent dissipation rate. The time step used in the simulations was initially 0.0001 s, and it gradually increased to 0.001s. Convergence was achieved when residuals on continuity, velocities, kinetic energy and energy dissipation rate became less than 10^{-3}.

Data Processing

In this study, simulation results mainly focused on the water flow depth and the velocity distribution in spiral concentrators. Holland-Batt defined the water depth in a spiral concentrator as the thickness of the water flow at the bottom of a vertical slot (Holland-Batt 1989). Loveday also suggested that the vertical thickness of water flow could be regarded as the water flow depth (Loveday and Cilliers 1994). In this paper, the Holland-Batt`s suggestion was adopted. Besides, the cross-section of the spiral trough was divided into 12 streams for a better description of the velocity distribution. The fraction of water depth, h_f, was defined to describe the relative position along the direction of water depth. Figure 2 shows the schematic diagram of the flow depth, the streams across the trough, and the fraction of water depth in a spiral concentrator.

The water flow depth (h_r) in a spiral concentrator can be calculated by the following formula:

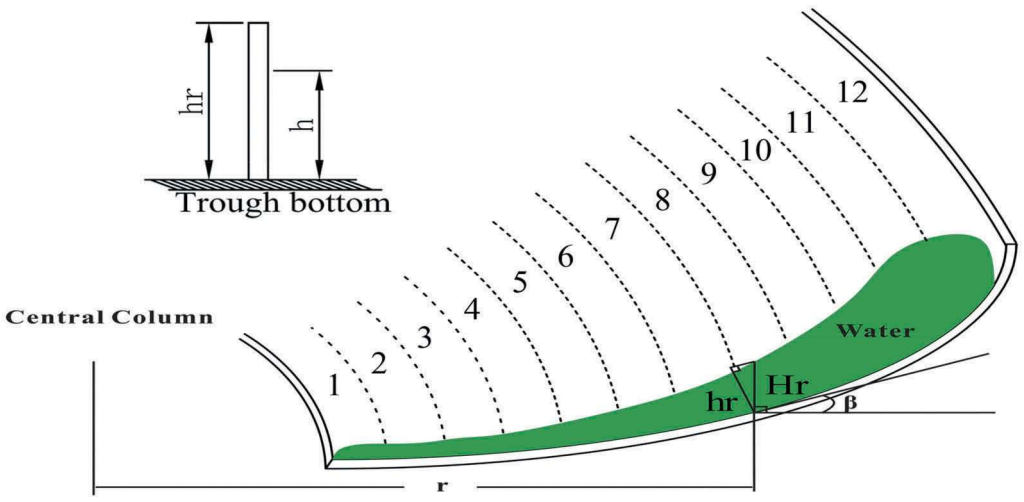

Figure 2. Schematic diagram of flow depth in a spiral concentrator.

$$h_r = H_r \times \cos\beta \quad (7)$$

where r stands for the radial distance from the central column, mm; H_r is the vertical flow depth, mm. H_r is perpendicular to the horizontal; h_r means the flow depth, mm. The h_r is the projection of H_r in the normal direction, which is perpendicular to the trough; β stands for the transverse angle.

The fractional depth, *hf*, was defined as the ratio of the position off the bottom (*h*) to the water depth (*hr)*.

Results and Discussion

Distribution of Water Flow Depth and Velocity in Spiral Concentrator

(1) Water flow depth

Compared with the inconvenient measurement of the secondary flow, the water flow depth was an easy-measured value. Generally, the water depth was usually taken as the criterion to verify the accuracy of simulation method (Doheim et al. 2008; Matthews, Fletcher, and Partridge 1998). Figure 3 shows the prediction of water depth in the LD-9 spiral concentrator at the flow rate of 8 m^3/h. Experimental findings of water depth were collected by Holland-Batt (Holland-Batt 1989).

As shown in Fig. 3, the flow depth increases radially outwards, which is consistent with the previous findings (Doheim et al. 2008; Holland-Batt 1989). The predictions of water depth with the Standard k-ϵ model, the RNG k-ϵ model, and the Reynolds-stress model (RSM) show agreement with experimental measurements. As presented by the software Theory Guide, RSM has great potential to give accurate predictions for complex flows with streamline curvature, swirl, rotation, and rapid changes in strain rate (ANSYS Fluent 2013). Figure 3(b) also shows that the RSM model is superior to other turbulence model. The RSM is suggested in subsequent numerical experiments.

(2) Distribution of velocity

Distribution of velocity in spiral concentrators mainly referred to the primary flow velocity distribution and the secondary flow distribution (Holland-Batt 1989; Holtham

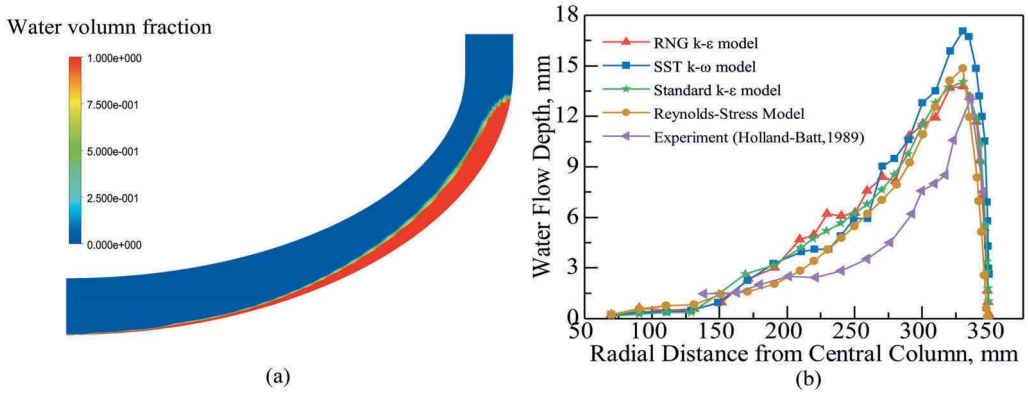

Figure 3. Water flow depth: (a)-contour map; (b)-experimental results versus numerical prediction.

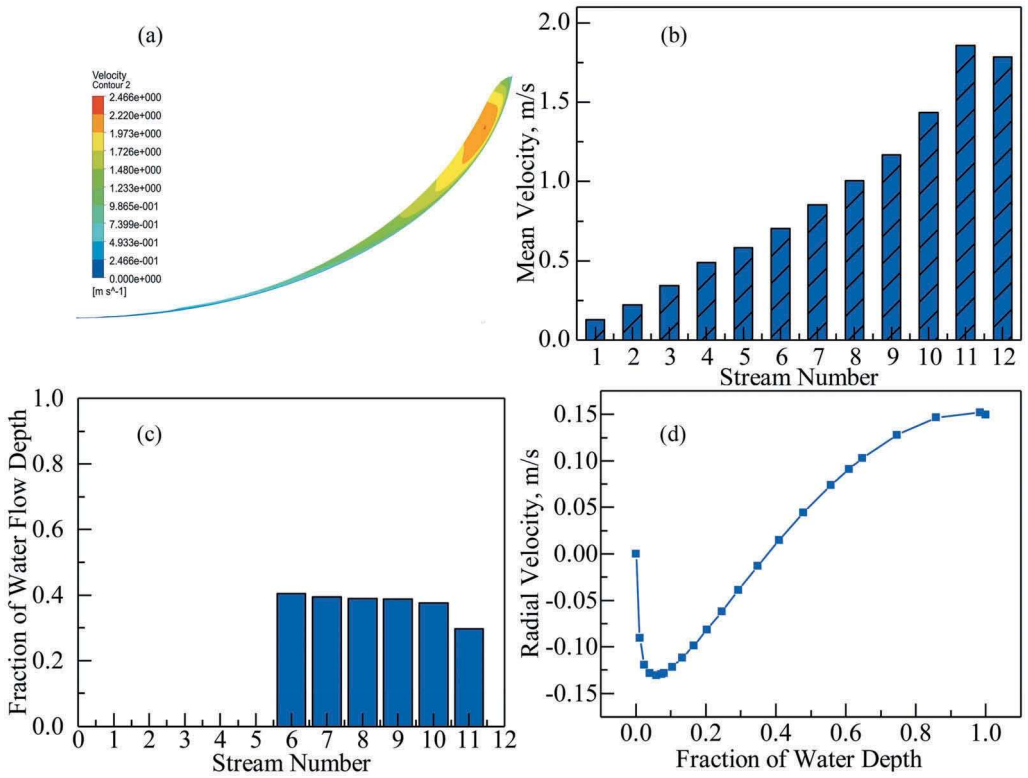

Figure 4. Predicted velocity distribution: (a) contour map; (b) mean velocity; (c/d) secondary flow.

1990a, 1992, 1990b; Jain and Rayasam 2017; Loveday and Cilliers 1994). Figure 4 shows the predicted velocity distribution in the LD-9 spiral concentrator at the flow rate of 8 m^3/h.

The contour map in Fig. 4(a) shows the primary flow velocity distribution in the LD-9 spiral concentrator. Figure 4(b) shows the mean primary velocity of each stream across the trough profile. Figure 4(c) shows distribution of the reversal position, where the water flow reversal occurs in spiral concentrators. Figure 4(d) gives the detail radial velocity distribution of the stream 10. As illustrated in Fig. 4, the primary velocity across thetrough increases with radial distance from the central column, which is consistent with the experimental findings (Holland-Batt 1989; Loveday and Cilliers 1994). the secondary flow in spiral concentrator is discontinuous. The reversal position of the secondary in outer region of the trough is approximate at the fractional depth of 0.4. Attributed to the visualization of the flow field, it is convenient to investigate the effect of design parameterson water flow field in spiral concentrators using the CFD methods.

Effect of Design Parameters on Water Flow Depth

The previous studies have confirmed that the water flow depth in spiral concentrators accumulated outwards (Doheim et al. 2008; Holland-Batt 1989; Holtham 1990a; Loveday and Cilliers 1994; Matthews, Fletcher, and Partridge 1998; Matthews et al. 1999). Figure 5

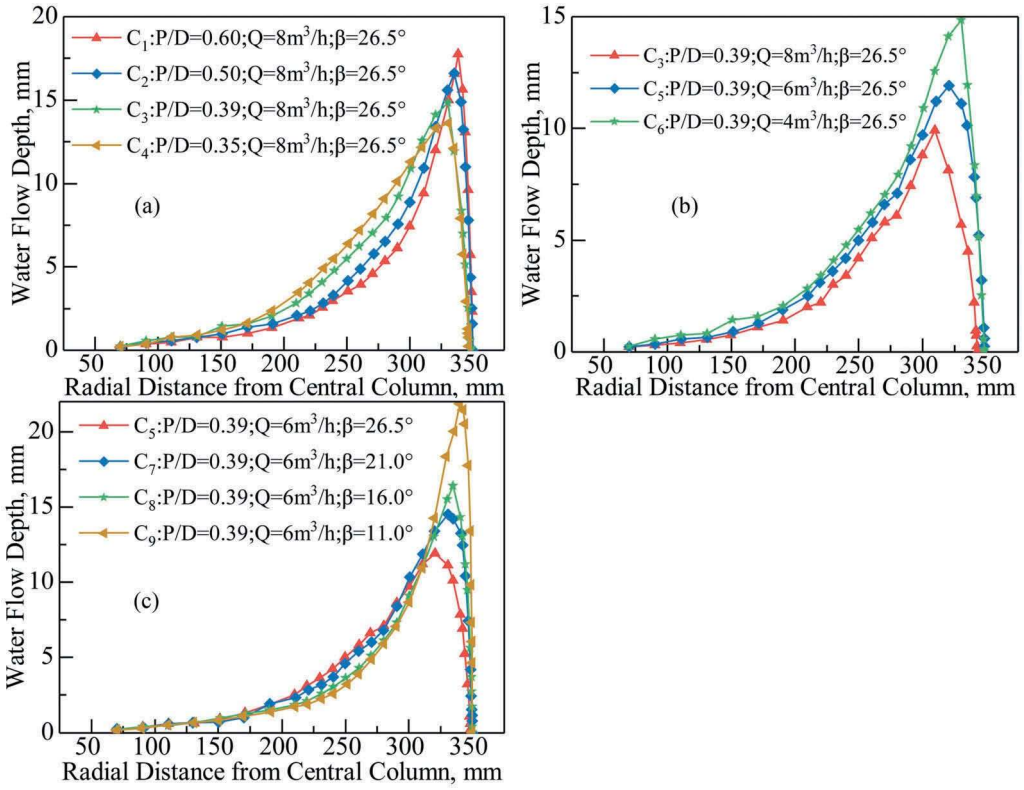

Figure 5. Impact of parameters on water flow depth: (a) Pitch; (b) Flow Rate; (c) Transverse Angle.

shows the comparison of the predicted water depth in numerical experiments with different design factors.

The data plotted in Fig. 5 show that the water flow depth increases radially outwards. The design parameters have little effect on water depth in the inner region of the trough.

Specifically, the flow depth in the middle of the trough increases with the decrease of the pitch and the transverse angle. The reduction of the pitch and the transverse angle in the outer region of the trough decrease the water depth in the outer zone. The water velocity in spiral concentrator with high pitch is much higher than that in spiral concentrator with a low pitch, because the high pitch indicates that the transformation of the gravitational potential energy into kinetic energy is high. Hence, increasing the pitch will make it easier for water to move outward. The steep trough is an obstruction for the water to move outwards. Increasing the transverse angle indicates the difficulty for water to move outwards. As shown in Fig. 5(c), a remarkable decrease of water depth occurs in the outer trough when decreasing the transverse angle. Therefore, careful consideration of the trough transverse angle needs to be taken into when designing the spiral concentrator.

Furthermore, the water depth increases with the flow rate, especially in the outer region of the trough. There is a minor increase of the water flow depth in the inner and middle zone as the flow rate increases, which shows agreement with the experimental findings

(Glass, Minekus, and Dalmin 1999). This unique water depth distribution is the possible reason for the stability of separation during the fluctuating flow rate.

Effect of Design Parameters on Mean Primary Velocity

The mean primary velocity was normally used to describe the primary velocity distribution in spiral concentrators (Holland-Batt 1989; Holtham 1992). Currently, the effects of designfactors on the primary velocity has not been investigated. Figure 6 shows the comparisonof the mean primary velocity in numerical experiments.

The bar charts in Fig. 6 shows that the mean primary velocity across the trough increases gradually with the radial distance from the central column. The pitch and the flow rate mainly affect the mean primary velocity in the outer trough. The transverse angle has an obvious effect on the mean primary velocity both in the inner and outer trough.

To be specific, both the pitch and the flow rate have little influence on the mean primary velocity of stream 1 ~ 10. The mean velocity in stream 1 ~ 10 increases approximatively with the decrease of the pitch and the increase of the flow rate. Whereas the pitch and the flow rate have an obvious influence on the mean primary velocity in the outer zone. High pitch and flow rate indicate the high mean velocity in stream 11 ~ 12.

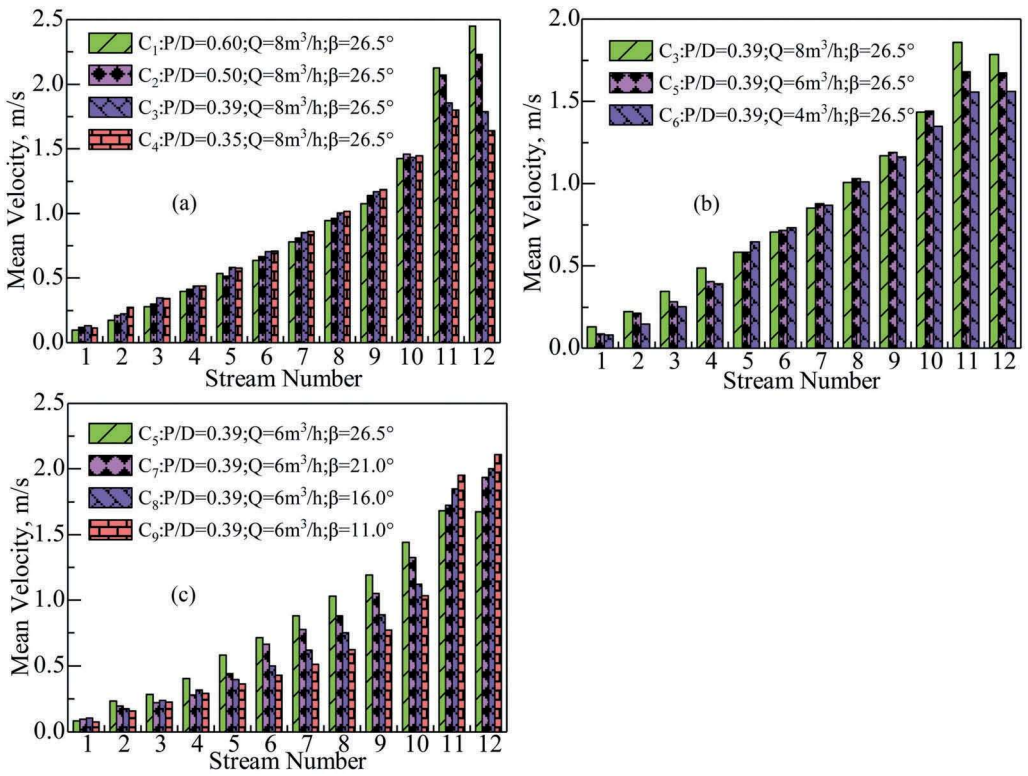

Figure 6. Effect of parameters on primary velocity: (a) Pitch; (b) Flow Rate; (c) Transverse Angle.

Moreover, the mean primary velocity of stream 2 ~ 10 decreases with the transverse angle. The high transverse angle makes it difficult for water to move outwards. As discussed in Fig. 5, the flow depth in stream 11 ~ 12 decreases as the transverse angle increases. For the spiral concentrator with the large transverse angle, much water should flow from stream 2 ~ 10 since the total volume of water flowing from the stream 11 ~ 12 decreases. However, Fig. 5 has shown that the transverse angle has no obvious influenceon the water depth in stream 2 ~ 10. Hence, the mean primary velocity in stream 2 ~ 10 is sensitive to the transverse angle. Therefore, the transverse angle of the trough should be considered carefully during the design progress.

Effect of Design Parameters on Secondary Flow

Because of the friction resistance near the bottom of the trough, the primary velocity of the water near the trough is smaller than that of the water closed to the free-surface (Matthews et al. 1999). As a result, the centrifugal force, acting on the water in the upper layers, take the domain position and force the water to move outwards. In contrast, the water near the trough prefers to move inward since the gravity and the friction force arethe major forces compared with the centrifugal force (Jain and Rayasam 2017; Kapur and Meloy 1998). Consequently, the secondary flow is generated. Little information about the velocity reversal position and the intensity of the secondary flow has been discussedbefore. Figure 7 shows the reversal positions of each stream in numerical experiments.

As shown in Fig. 7, the distribution of secondary flow is discontinuous. No obvious secondary flow exists in the inner region of the trough. To some extent, the primary velocity and water depth in the inner region are too small to generate the secondary flow. The wash-water addition in the inner region of the trough may be an evidence for the

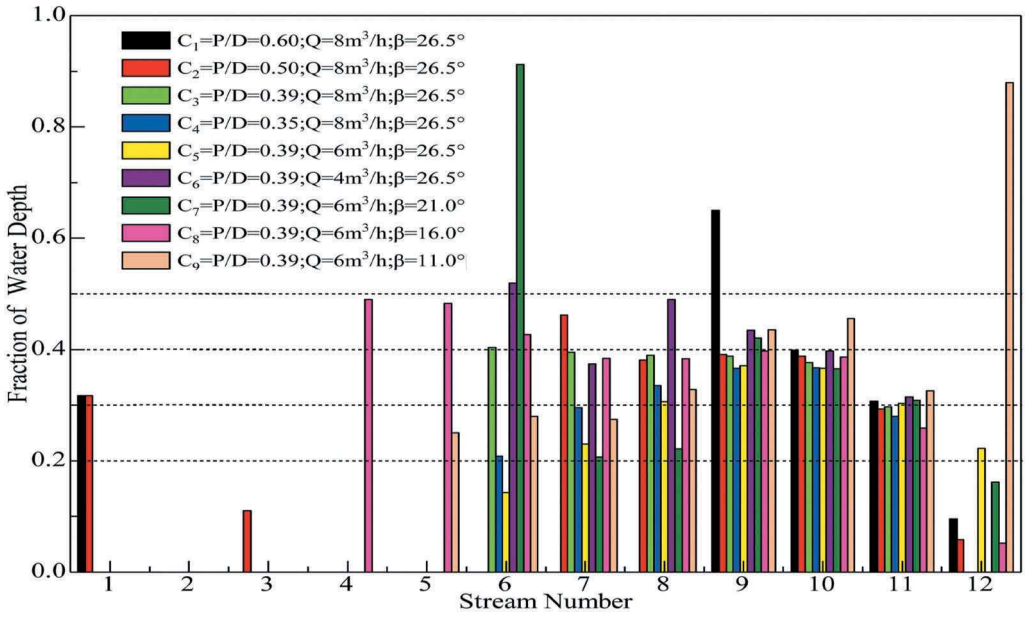

Figure 7. Effect of design parameters on reversal position.

discontinuous secondary flow (Dehaine and Filippov 2016). Besides, Loveday has detected that the abnormal secondary flow existed in the inner trough (Loveday and Cilliers 1994). This could be taken as another proof of the discontinuous secondary flow in the inner region of the trough.

Besides, the design parameters have a significant influence on the reversal position. In general, the reversal position is approximate at the fractional depth of 0.2 ~ 0.5. When the P/D, Q, and transverse angle were 0.39, 6 m^3/h, and 16.0°, respectively, the secondary flow in the spiral concentrator covers the widest area across the trough among the nine simulation results.

Further investigation for the effect of design factors on the secondary velocity (radial velocity) was conducted by comparison the prediction radial velocity of the stream 10. The effect of design factors on the radial velocity of stream 10 is illustrated in Fig. 8.

Combined the Fig. 6 and the Fig. 8, it is apparent that the secondary velocity is smaller than the primary velocity. Figure 8 also shows that the secondary velocity increases with the reduction of the pitch and the flow rate. Besides, the secondary velocity increases with the transverse angle. It has been reported that the water flow in the outer region was the turbulence flow (Doheim et al. 2008; Holland-Batt 1989). As discussed in Fig. 6, spiral concentrators with high pitch, high flow rate, or low transverse angle can increase the mean primary velocity in the outer region of the trough, which indicated that the turbulenceflow in outer trough are strengthened. The enhancement of the turbulence flow can affect the generation of the secondary flow. Hence, the low secondary velocity occurs in spiral

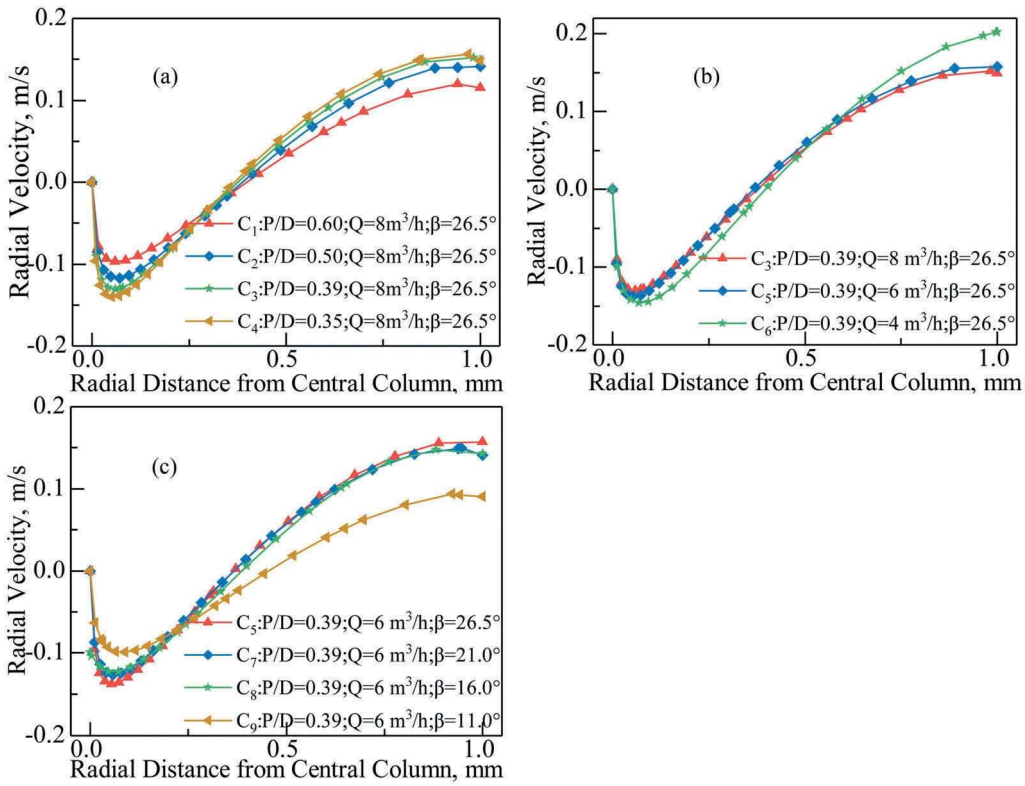

Figure 8. Effect of parameters on the secondary velocity of stream 10.

concentrators with high pitch, high flow rate, or low transverse angle. That being said, it may be inadvisable for these mineral particles with light density to use the spiral concentrator with high pitch, high flow rate, or low transverse angle, because it will be tough to force the particle near the bottom to move inward due to the weak secondary flow.

Conclusions

The overall objective of this study was to explore the water flow field distribution and the effect of the design parameters on the water flow field in spiral concentrators. The main conclusions can be drawn as follows:

(1) The Reynolds-Stress Model (RSM) turbulence model is superior to other turbu- lence models. The water flow depth and the primary velocity increase radially outwards. The secondary velocity is relatively small compared with the primary velocity.
(2) The design factors mainly influence the water depth in the outer trough. The pitch and the flow rate have little effect on the primary velocity in inter and middle zoneof the trough, while the transverse angle has an obvious influence on the mean primary velocity both on the inner and outer trough.
(3) The secondary flow in spiral concentrator is discontinuous, and hardly any secondary flow exists near the central column. The reversal position is approximate at the fractional depth of 0.2 ~ 0.5. The reduction of the pitch and the flow rate, together with the increase of the transverse angle, can strengthen the secondary flow.

Acknowledgments

Thanks for the financial support provided by the National Natural Science Foundation of China (Grant No. 51504262). Guichuan Ye also wants to acknowledge the financial support (Grant No. 201706430054) from China Scholarship Council (CSC) for his visiting study at the University of Birmingham.

Funding

This work was supported by the China Scholarship Council [201706430054];National NaturalScience Foundation of China [51504262].

References

ANSYS Fluent. 2013. *ANSYS Fluent Theory Guide, ANSYS, Inc.*, 275 Technology Drive Canonsburg, PA 15317.

Arnold, D. J., Y. M. Stokes, and J. E. F. Green. 2014. Thin-film flow in helically-wound rectangular channels of arbitrary torsion and curvature. *Journal of Fluid Mechanics* 764:76–94. doi:10.1017/jfm.2014.703.

Bazin, C., M. Sadeghi, M. Bourassa, P. Roy, F. Lavoie, D. Cataford, C. Rochefort, and C. Gosselin. 2014. Size recovery curves of minerals in industrial spirals for processing iron oxide ores.*Minerals Engineering* 65:115–23. doi:10.1016/j.mineng.2014.05.012.

Boucher, D., Z. Deng, T. Leadbeater, R. Langlois, M. Renaud, and K. E. Waters. 2014. PEPT studies of heavy particle flow within a spiral concentrator. *Minerals Engineering* 62:120–28. doi:10.1016/j.mineng.2013.12.022.

Boucher, D., Z. Deng, T. Leadbeater, R. Langlois, and K. E. Waters. 2016a. Observation of iron ore beneficiation within a spiral concentrator by positron emission particle tracking of large (Ø=1440μm) and small (Ø=58μm) hematite and quartz tracers. *Chemical Engineering Science* 140:217–32. doi:10.1016/j.ces.2015.10.018.

Boucher, D., Z. Deng, T. W. Leadbeater, R. Langlois, and K. E. Waters. 2016b. Speed analysis of quartz and hematite particles in a spiral concentrator by PEPT. *Minerals Engineering* 91:86–91. doi:10.1016/j.mineng.2015.09.014.

Brackbill, J. U., D. B. Kothe, and C. Zemach. 1992. A continuum method for modeling surface tension. *Journal of Computational Physics* 100:335–54. doi:10.1016/0021-9991(92)90240-Y.

Das, S. K., K. M. Godiwalla, L. Panda, K. K. Bhattacharya, R. Singh, and S. P. Mehrotra. 2007. Mathematical modeling of separation characteristics of a coal-washing spiral. *International Journal of Mineral Processing* 84:118–32. doi:10.1016/j.minpro.2007.05.007.

Dehaine, Q., and L. O. Filippov. 2016. Modelling heavy and gangue mineral size recovery curves using the spiral concentration of heavy minerals from kaolin residues. *Powder Technology* 292:331–41. doi:10.1016/j.powtec.2016.02.005.

Dixit, P., R. Tiwari, A. K. Mukherjee, and P. K. Banerjee. 2015. Application of response surface methodology for modeling and optimization of spiral separator for processing of iron ore slime. *Powder Technology* 275:105–12. doi:10.1016/j.powtec.2015.01.068.

Doheim, M. A., A. F. Abdel Gawad, G. M. A. Mahran, M. H. Abu-Ali, and A. M. Rizk. 2008. Computational prediction of water-flow characteristics in spiral separators part I, flow depth and turbulence intensity. *Journal of Engineering Sciences,Assiut University* 36:935–50.

Doheim, M. A., A. F. Abdel Gawad, G. M. A. Mahran, M. H. Abu-Ali, and A. M. Rizk. 2013. Numerical simulation of particulate-flow in spiral separators: Part I. Low solids concentration (0.3% & 3% solids). *Applied Mathematical Modelling* 37:198–215. doi:10.1016/j.apm.2012.02.022.

Ganegama Bogodage, S., and A. Y. T. Leung. 2015. CFD simulation of cyclone separators to reduce air pollution. *Powder Technology* 286:488–506. doi:10.1016/j.powtec.2015.08.023.

Glass, H. J., N. J. Minekus, and W. L. Dalmin. 1999. Mechanics of coal spirals. *Minerals Engineering* 12:271–80. doi:10.1016/S0892-6875(99)00005-9.

Grobler, J. 2017. The influence of trash minerals and agglomerate particles on spiral separation performance. *Journal of the Southern African Institute of Mining and Metallurgy* 117:435–42. doi:10.17159/2411-9717/2017/v117n5a5.

Hirt, C. W., and B. D. Nichols. 1981. Volume of fluid (VOF) method for the dynamics of free boundaries. *Journal of Computational Physics* 39:201–25. doi:10.1016/0021-9991(81)90145-5.

Holland-Batt, A. B. 1989. Spiral separation: Theory and simulation. *Transactions of the Institution of Mining and Metallurgy, Section C* 98:46–60.

Holland-Batt, A. B. 1995. The dynamics of sluice and spiral separations. *Minerals Engineering* 8:3–21. doi:10.1016/0892-6875(94)00098-W.

Holland-Batt, A. B. 2009. A method for the prediction of the primary flow on large diameter spiral troughs. *Minerals Engineering* 22:352–56. doi:10.1016/j.mineng.2008.10.002.

Holtham, P. N. 1990a. *The fluid flow pattern and particle motion on spiral separators* (doctoral dissertation). Australia: University of New South Wales.

Holtham, P. N. 1990b. Flow visualisation of secondary currents on spiral separators. *Minerals Engineering* 3:279–86. doi:10.1016/0892-6875(90)90123-S.

Holtham, P. N. 1992. Primary and secondary fluid velocities on spiral separators. *Minerals Engineering* 5:79–91. doi:10.1016/0892-6875(92)90007-V.

Jain, P. K., and V. Rayasam. 2017. An analytical approach to explain the generation of secondary circulation in spiral concentrators. *Powder Technology* 308:165–77. doi:10.1016/j.powtec.2016.11.040.

Kapur, P. C., and T. P. Meloy. 1998. Spirals observed. *International Journal of Mineral Processing* 53:15–28. doi:10.1016/S0301-7516(97)00053-7.

Kwon, J., H. Kim, S. Lee, and H. Cho. 2017. Simulation of particle-laden flow in a humphrey spiral concentrator using dust-liquid smoothed particle hydrodynamics. *Advanced Powder Technology* 28:2694–705. doi:10.1016/j.apt.2017.07.022.

Li, M., C. J. Wood, and J. J. Davis. 1993. A study of coal washing spirals. *Coal Preparation* 12:117–31. doi:10.1080/07349349308905113.

Loveday, G. K., and J. J. Cilliers. 1994. Fluid flow modelling on spiral concentrators. *Minerals Engineering* 7:223–37. doi:10.1016/0892-6875(94)90066-3.

Matthews, B., C. Fletcher, A. Partridge, and S. Vasquez. 1999. Computations of curved free surface water flow on spiral concentrators. *Journal of Hydraulic Engineering* 125:1126–39. doi:10.1061/(ASCE)0733-9429(1999)125:11(1126).

Matthews, B. W., C. A. J. Fletcher, and A. C. Partridge. 1998. Computational simulation of fluid and dilute particulate flows on spiral concentrators. *Applied Mathematical Modelling* 22:965–79. doi:10.1016/S0307-904X(98)10030-6.

Matthews, B. W., C. A. J. Fletcher, and A. C. Partridge 1999. Particle flow modeling on spiral concentrators, benefits of dense media for coal Processing: Benefits of dense media for coal processing? Second International Conference on CFD in the Minerals and Process Industries. Melbourne, Australia: CSIRO, December 6–8.

Mishra, B. K., and A. Tripathy. 2010. A preliminary study of particle separation in spiral concentrators using DEM. *International Journal of Mineral Processing* 94:192–95. doi:10.1016/j.minpro.2009.12.005.

Palmer, M. K. 2016. The development of a new low cut point spiral for fine coal processing. XVIII International Coal Preparation Congress, 861–66. Springer, Cham.

Song, T., K. Jiang, J. Zhou, D. Wang, N. Xu, and Y. Feng. 2015. CFD modelling of gas–Liquid flow in an industrial scale gas-stirred leaching tank. *International Journal of Mineral Processing* 142:63–72. doi:10.1016/j.minpro.2015.01.005.

Tripathy, S. K., and Y. Rama Murthy. 2012. Modeling and optimization of spiral concentrator for separation of ultrafine chromite. *Powder Technology* 221:387–94. doi:10.1016/j.powtec.2012.01.035.

Wadnerkar, D., M. O. Tade, V. K. Pareek, and R. P. Utikar. 2016. CFD simulation of solid–Liquid stirred tanks for low to dense solid loading systems. *Particuology* 29:16–33. doi:10.1016/j.partic.2016.01.012.

Wang, J., and J. R. G. Andrews. 1994. Numerical simulations of liquid flow on spiral concentrators. *Minerals Engineering* 7:1363–85. doi:10.1016/0892-6875(94)00076-X.

Xu, Q., J. Feng, and S. Zhang. 2017a. Effects of different loads on structure stress of “L”-type large-diameter pipeline under burying and trench conditions based on fluid–Structure–Heat coupling. *International Journal of Heat and Mass Transfer* 115:387–97. doi:10.1016/j.ijheatmasstransfer.2017.07.052.

Xu, Q., J. Feng, and S. Zhang. 2017b. Combined effects of different temperature and pressure loads on the “L”-type large-diameter buried pipeline. *International Journal of Heat and Mass Transfer* 111:953–61. doi:10.1016/j.ijheatmasstransfer.2017.04.067.

Youngs, D. L. 1982. Time-dependent multi-material flow with large fluid distortion. In *Numerical methods in fluid dynamics*, ed. K. W. Morton and M. J. Baines, 273–85. New York, NY: Academic Press.